



FTO modulates circadian rhythms and inhibits the CLOCK-BMAL1-induced transcription



Chao-Yung Wang^{a,*}, Shian-Sen Shie^b, I-Chang Hsieh^a, Ming-Lung Tsai^a,
Ming-Shien Wen^a

^a Department of Cardiology, Chang Gung Memorial Hospital and Chang Gung University College of Medicine, Taiwan

^b Department of Infectious Diseases, Chang Gung Memorial Hospital and Chang Gung University College of Medicine, Taiwan

ARTICLE INFO

Article history:

Received 7 July 2015

Accepted 8 July 2015

Available online 15 July 2015

Keywords:

Circadian rhythm

FTO

Transcription

CLOCK

BMAL1

ABSTRACT

Variations in the human fat mass and obesity-associated gene, which encodes FTO, an 2-oxoglutarate-dependent nucleic acid demethylase, are associated with increased risk of obesity. These FTO variations were recently shown to affect IRX3 and the exact function of FTO is still controversial. Obesity is closely linked to circadian rhythm. To understand the role of FTO in circadian rhythm, we analyzed the circadian rhythm of FTO deficient mice. FTO deficient mice had robust circadian locomotor activity rhythms with prolonged periods. The light-induced phase shifts of circadian rhythms were also significantly affected in FTO deficient mice. Tissue explants of FTO deficient mice maintained robust peripheral rhythms with prolonged period. Overexpress of FTO represses the transcriptional activation by CLOCK and BMAL1. Core clock genes expression of mRNA and protein were also altered in FTO deficient mice. Furthermore, FTO co-immunoprecipitated with CRY1/2 in a circadian manner. These results indicate a fundamental link between the circadian rhythm and FTO and extend the function of FTO to the core clockwork machinery.

© 2015 Elsevier Inc. All rights reserved.

1. Introduction

Fat mass and obesity-associated (FTO) is a 2-oxoglutarate-dependent nucleic acid demethylase [1]. In 2007, genome-wide association studies identified single nucleotide polymorphisms (SNP) in intron 1 of *FTO* associated with an increased risk of adult obesity [2]. Individuals homozygous for *FTO* risk alleles weigh approximately 3 kg more than individuals without risk alleles [3]. Later, this association was also identified in additional global studies of different ethnicities [4]. These *FTO* variants are recently shown to interact with iroquois-class homeodomain protein IRX-3 [5] or Retinitis Pigmentosa GTPase Regulator-Interacting Protein-1 Like (RGRIP1L) [6]. Mice with increased *FTO* levels displayed increased energy intake and increased adiposity [7]. Loss-of-function mutations in the *FTO* gene in humans [8] or mice [9] result in severe growth impairment and multiple abnormalities in the brain and heart, in addition to facial dysmorphism, indicating a more fundamental role of FTO in human physiology.

Previous studies have supported the hypothesis that FTO has

additional diverse roles besides its involvement in obesity. FTO is ubiquitously expressed, with the highest expression observed in the brain [10]. FTO deficient cells cannot sense amino acids and respond by reducing mammalian target of rapamycin (mTOR) signaling and increasing autophagy [11]. Functional magnetic resonance imaging (MRI) studies have shown that the *FTO* genotype modulates neural responses to food through the gut hormones, ghrelin [12]. Together, these studies describe the complexity and existence of distinct interacting factors that mediate FTO function. Indeed, this hypothesis is also supported by the fact that FTO targets only a specific subset of m⁶A-modified mRNAs [13]. Nevertheless, the identities of other factors that interact with FTO are unknown.

Circadian clocks drive endogenous rhythms of hormonal, behavioral, sleep, and metabolic physiological functions and coordinate with environmental light, food, and temperature inputs. Disturbed circadian rhythms result in metabolic syndrome, increased incidence of cancer, and cardiovascular diseases [14]. Molecular circadian clocks function via a transcription and translation feedback loop. Heterodimers of circadian locomotor output cycles kaput (CLOCK) and brain and muscle ARNT-like 1 (BMAL1) drive the rhythmic transcription of three *Period* genes (*PER1–3*) and two cryptochrome genes (*CRY1* and *CRY2*) from circadian E-box

* Corresponding author. 5 Fu-Hsing Street, Taoyuan 333, Taiwan.
E-mail address: cwang@ocean.ag (C.-Y. Wang).

elements. The PER/CRY protein complexes then translocate back into nucleus to inhibit CLOCK:BMAL1-mediated transcription. The full cycle of transcription, translation, and feedback inhibition takes 24 h to complete [15]. Several lines of evidence have supported that circadian clocks have close interactions with metabolism. Genetic disruption of clock genes in mice results in metabolic disturbances and shift work leads to metabolic syndromes [16]. However, the exact links between obesity and circadian rhythm are still unclear. Here, we hypothesize that FTO plays important role in circadian rhythm and studied the role of FTO in circadian machinery.

2. Material and methods

2.1. Cells, plasmids, and antibodies

Wild-type and *FTO*^{-/-} MEF cultures were established from E13.5 embryos and cultured with DMEM and 10% FBS. Full-length *FTO* cDNA were amplified by PCR from human adipocyte cell lines (PromoCell) or C57BL/6J mouse adipocytes. *BMAL1-luc* reporter

[17], *Rev-Erb α -luc* reporter [18], *DBP-luc* reporter [18], *PER1-luc* reporter [19], and *Rev-Erb α* expression [20] vectors were generous gifts from Dr. Hogenesch, Dr. Schibler, Dr. Reppert, Dr. Weaver, and Dr. Takumi, respectively. Antibodies used for immunoblotting and immunofluorescence included anti-FTO (Abnova, Neihu, Taiwan, PAB11419), anti-CRY1/2 (Alpha Diagnostic, San Antonio, TX, USA), anti-BMAL1 (Millipore, Billerica, MA, USA), anti-CLOCK (Calbiochem, Billerica, MA, USA), anti-PER1/2 (Millipore), anti-Rev-Erb α (Cell Signaling Technology, Danvers, MA, USA), anti-V5 (Invitrogen), anti-HA (Roche, Indianapolis, IN, USA), and anti-Flag M2 (Sigma, St. Louis, MO, USA) antibodies.

2.2. Purification of FTO complexes

To obtain Flag-FTO-HA-expressing cell lines, HeLa cells were transfected with pCMV-Flag-FTO-HA and selected for 2 weeks in G418. We selected clones 1 and 4, which had similar native and overexpressed FTO levels, for further experiments. Cells (5×10^9) were lysed and isolated nuclear lysates were immunoprecipitated

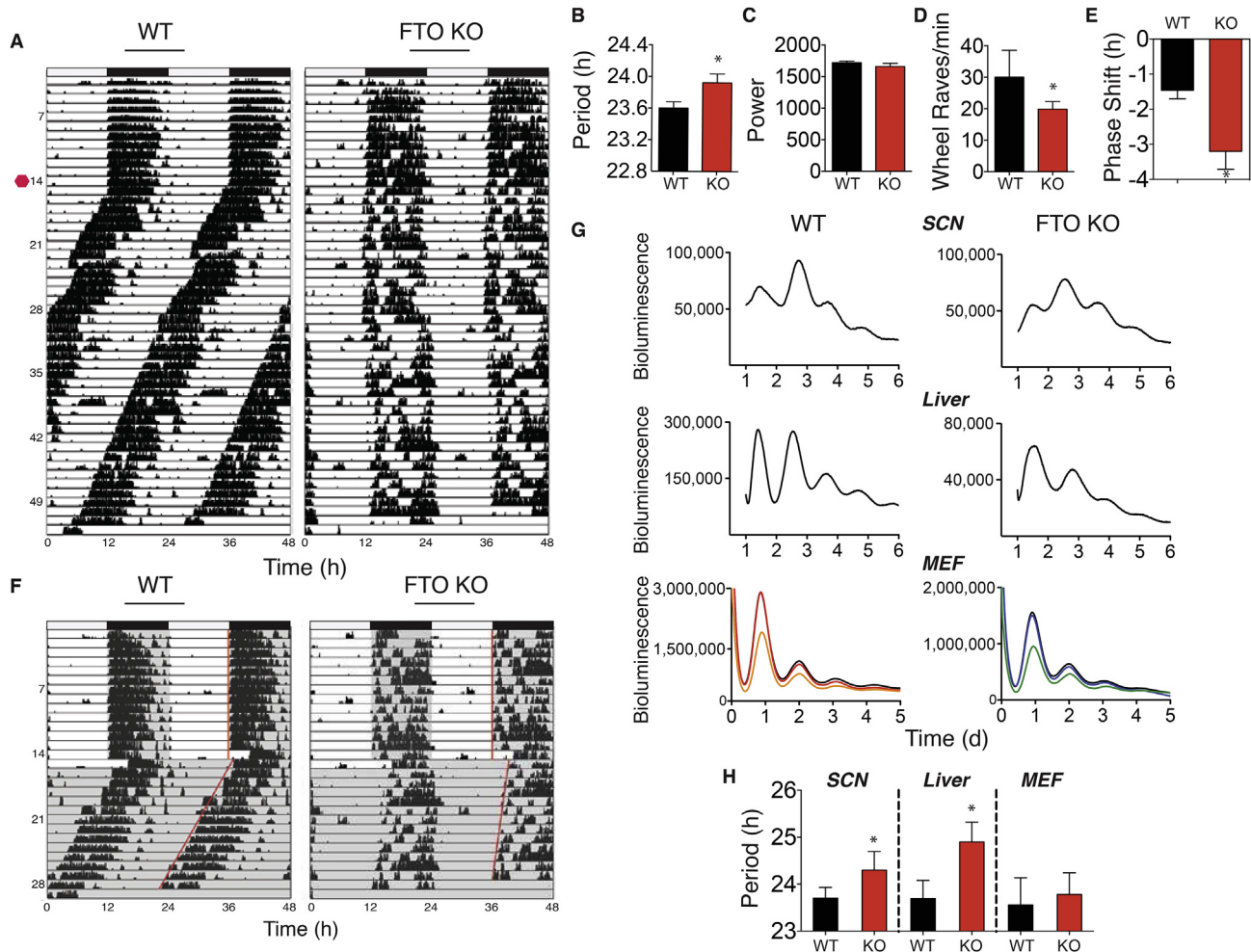


Fig. 1. FTO deficient mice maintained locomotor activity rhythms with a lengthened circadian period. (A) Representative activity records (actograms) of wild-type mice (WT) and FTO deficient mice (FTO KO) are shown in a double-plotted format. Each horizontal line represents 48 h; the second 24-h period is plotted to the right and below the first. The mice were initially kept on a 12-h light:12-h dark cycle (LD) and were then transferred to constant darkness (DD; indicated by the red hexagon). Numbers on the left indicate days of the study. (B) Periodogram estimates of periods. Each bar represents the mean \pm SD; $n = 12$ in each group. * $P < 0.05$. (C) Circadian amplitude (power from periodogram calculation). $P = 0.53$. (D) Activity levels during the DD phase. * $P < 0.05$. (E) The phase shifts for WT ($n = 11$) and FTO deficient mice ($n = 4$). * $P < 0.001$. (F) Response to light from CT 12–16. Representative double-plotted activity records from WT and FTO deficient mice. Mice were initially kept on a 12-h light:12-h dark cycle (LD). The lights were then left on from CT 12–16, followed by exposure to constant darkness (DD). The red lines mark the phase of activity onset before and after the light manipulation. (G) Representative records of bioluminescence showing circadian profiles of mPER2 levels from the SCN, liver, and MEFs of WT or FTO deficient *mPer2^{Luc}* mice. Each bar represents the mean \pm SD; $n = 6$ in each group. * $P < 0.05$. (H) Period values of mPER2 rhythms in the SCN, liver, and MEFs. * $P < 0.05$. (For interpretation of the references to color in this figure legend, the reader is referred to the web version of this article.)

using anti-Flag M2 agarose. Precipitate was eluted using the Flag peptide and immunopurified using anti-HA antibody-conjugated agarose. Protein bands were subjected to concerted matrix-assisted laser desorption ionization (MALDI) peptide mass fingerprinting and collision-induced fragmentation MS/MS analysis by the Core Facilities for Protein Structural Analysis located at the Institute of Biological Chemistry, Academia Sinica.

2.3. Animals and collection of liver tissues

Embryonic stem cells and mice with loxP sites surrounding FTO exon 3 were obtained from EUCOMM (Institute of Developmental Genetics) and Mouse Genetics Programme (Wellcome Trust Sanger Institute). FTO deficient mice were generated from matings between FTO^{loxP/loxP} mice and Ella-cre mice. Homozygous FTO deficient mice and wild-type mice were generated from matings between two heterozygous mice. The animals were maintained on a 12-h light:12-h dark (LD) cycle (lights on at 7:00 AM and lights off at 7:00 PM). For circadian tissue collection, male mice were entrained on an LD cycle for 2 weeks and then transferred to constant darkness. Mice were sacrificed at the indicated circadian times. Tissues and organs were dissected under light and frozen in liquid nitrogen. The animal experiments were performed in accordance with the guidelines of Chang Gung University and Chang Gung Memorial Hospital Institutional Animal Care and Use Committee.

2.4. Behavioral analysis

Mice were housed individually in running wheel cages (Actimetrics, Wilmette, IL, USA) and maintained in light-controlled closets within an animal facility with temperature and humidity

controls. Food and water were available ad libitum. The animals were kept on a 12-h light:12-h dark cycle for at least 14 days before behavioral experiments. Behavioral data were collected with a 5-min bin width. ClockLab software (Actimetrics) was used for double-plotted actograms, χ^2 periodograms, and phase-shift analyses. To determine the circadian phase responses, linear regressions were fit to the activity onsets for seven days before and after the light shift. The phase shift was calculated as the difference in extrapolated onset of activity on the day of the manipulation.

2.5. Real-time bioluminescence assays

FTO deficient mice were mated with *mPer2^{Luciferase}*-knock-in mice to create heterozygous FTO deficient mice on a homozygous *mPer2^{Luciferase}*-knock-in background [21]. Homozygous FTO deficient mice carrying the *mPer2^{Luciferase}*-knock-in allele (FTO^{-/-} *mPer2^{Luc}*) were generated by mating between heterozygous FTO deficient mice. Wild-type *mPer2^{Luc}* mice and FTO^{-/-} *mPer2^{Luc}* mice were sacrificed simultaneously within the first 2 h after lights-on. Brains, SCNs, hearts, lungs, and livers from the same animals were dissected and cultured. Organ explants were dissected to 3–5 mm² and placed individually in culture wells with luciferin. Luciferase activities were recorded for 1 min at 15-min intervals with an LM2400 luminometer (Hamamatsu). The first 24 h of data were excluded to avoid the initial surge of luciferase activity after the explant cultures. Explants with low levels (<6000 cpm) were excluded. The raw data were smoothed by an adjacent-averaging method. The peak was measured as the highest point of smoothed data. The period was computed as the mean between the peaks.

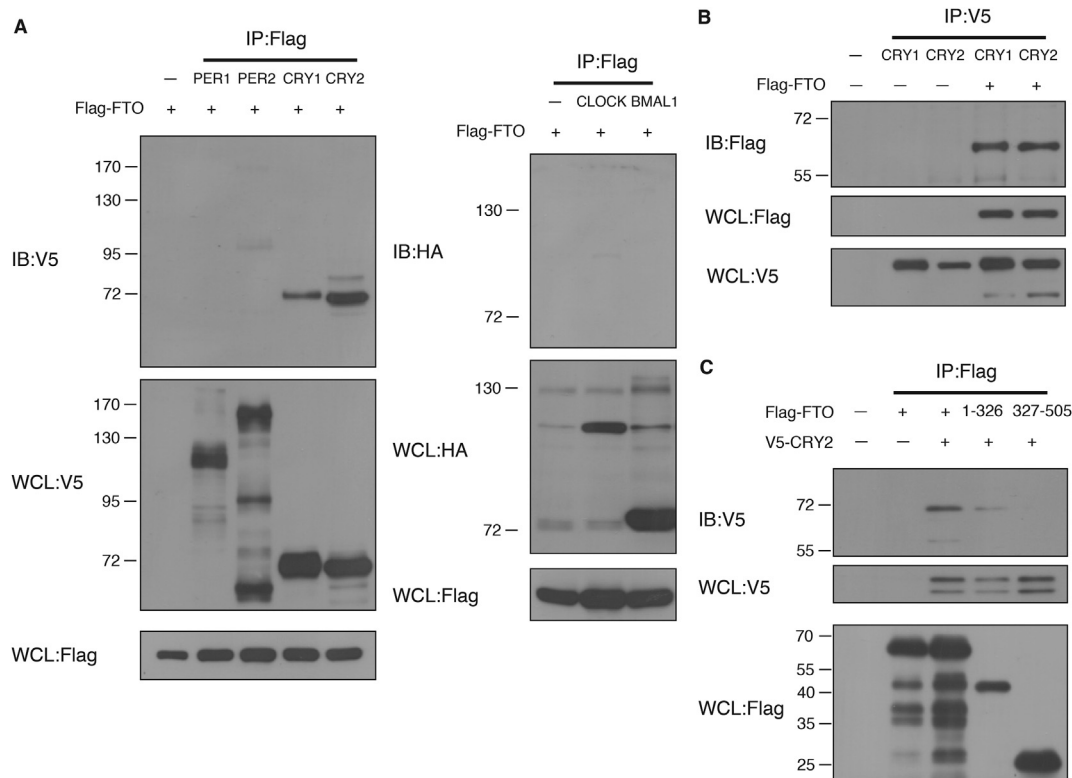


Fig. 2. FTO interacts with Cryptochrome. (A) Right: FTO interactions with PER1/2 and CRY1/2. 293T cells were transfected with V5-tagged PER1, PER2, CRY1, or CRY2 and Flag-tagged FTO. Whole cell lysates (WCLs) were analyzed by Flag immunoprecipitation and western blotting. Left: 293T cells were transfected with HA-CLOCK or HA-BMAL1 and Flag-FTO. Whole cell lysates (WCLs) were analyzed with Flag immunoprecipitation and western blotting. (B) Co-immunoprecipitation of FTO by V5-CRY1/2 from 293T WCLs. (C) Interaction of CRY2 with FTO N-terminal domain (1–326) analyzed by Flag immunoprecipitation and western blotting.

2.6. Transcriptional assays

Promoter activities were analyzed in MEFs and NIH3T3 cells. Cells (4×10^5) were seeded in 6-well plates and transfected with 25 ng *mPER1*, *mPER2*, or *Rev-Erb α* reporter plasmids with FuGENE 6 (Roche). One hundred nanograms CLOCK/BMAL1, 300 ng FTO, or 300 ng CRY2 plasmids were used as effector plasmids. The cells were lysed 48 h after transfection and analyzed with a dual-luciferase reporter assay system (Promega, Madison, WI, USA).

3. Results

3.1. Locomotor activity in FTO deficient mice

We monitored wheel-running activity of FTO deficient mice with an initial 14 days in a 12 h light/12 h dark (LD) cycle, followed by 4 weeks of constant darkness (DD). FTO deficient mice maintained robust circadian patterns of behavior, with periodicities that were on average about 18 min longer (23.9 ± 0.2 h; $n = 12$; mean \pm SD) than their wild-type siblings (23.6 ± 0.2 h; $n = 12$; Fig. 1A, B). All of the FTO deficient mice tested displayed prominent circadian rhythmicity throughout the 4 weeks in DD, comparable to that of their wild-type siblings (Fig. 1C), despite a significant reduction in their activity levels (Fig. 1D). Moreover, 14 of the 26 FTO deficient mice died during the wheel-running period, consistent with previous reports of early mortality in FTO deficient mice [9]. To further examine the responses of FTO deficient mice to light, we exposed wild-type and FTO deficient mice to LD for 2 weeks and then to a 4-h extension of the light period, followed by DD (Fig. 1E). After light exposure at circadian time (CT) 12–16, wild-type mice showed a phase delay of 1.5 ± 0.2 h, while FTO deficient mice showed a phase delay of 3.2 ± 1.4 h, 2 times longer than that of their wild-type siblings (Fig. 1F). To further assess FTO function in peripheral circadian oscillation, we generated FTO deficient mice carrying the *Per2^{Luciferase}* (*Per2^{Luc}*) allele, which allowed us to monitor circadian dynamics from tissue explants of wild-type and FTO deficient mice in real-time. Different tissues may have different peripheral circadian machinery, despite entrained by a master pacemaker in the suprachiasmatic nucleus (SCN) [22]. Using a real-time bioluminescence monitoring system, we found that isolated SCN, liver, and mouse embryonic fibroblasts (MEFs) from FTO deficient mice expressing the fusion *Per2::LUC* protein maintained self-sustained molecular oscillations in culture (Fig. 1G). Consistent with the wheel-running data, isolated SCN and liver from FTO deficient mice had longer period when compared to their wild-type counterparts. Isolated MEFs from FTO deficient mice tended to exhibit a longer oscillation period, but were not statistically significant (Fig. 1H). These results indicated that FTO was not required for the generation of robust circadian rhythms in locomotor activity and peripheral circadian oscillation. FTO deficiency resulted in altered responses to light and a prolonged circadian period.

3.2. FTO and CRY1/2 interactions in vivo

We then studied whether FTO could interact with PER1, PER2, CRY1, CRY2, BMAL1 and CLOCK. FTO copurified with CRY1 and CRY2, but not with PER1/2 (Fig. 2A) or CLOCK/BMAL1 (Fig. 2A, B). CRY2 bound the N-terminal domain of FTO but showed no affinity for its C-terminal domain (Fig. 2C). To avoid non-physiological interaction in the over-express system in cells, we generated modified HeLa cell lines that stably expressed FTO with N-terminal Flag and C-terminal HA epitopes (Supplementary Fig. 1A, 1B). Nuclear extracts from the stable cell lines were subjected to affinity chromatography on Flag-agarose beads and HA-affinity columns. FTO protein complexes were then analyzed by sodium dodecyl

sulphate (SDS)-polyacrylamide electrophoresis (Supplementary Fig. 1C). As expected, double-tagged FTO was a major component of the protein complex. We identified two major protein bands of ~500-kDa myeloid/lymphoid or mixed lineage leukemia 2 (MLL2) and 70-kDa CRY2 that copurified with ectopic FTO. Identification of CRY2 in the FTO protein complex further confirmed that FTO has important role in circadian rhythm modulation.

To determine the intracellular localization of the FTO-CRY interaction, we performed immunofluorescence staining in NIH-3T3 cells. Immunofluorescence confocal microscopy showed that CRY2 and FTO were colocalized in the nucleus (Fig. 3A). To further characterize the interaction between FTO and CRY1/2 *in vivo*, we immunoprecipitated liver nuclear extracts with anti-FTO antibodies from wide-type mice at different CTs. CRY1 and CRY2 copurified with FTO mainly at CT 13 and 17 (Fig. 3B). The levels of immunoprecipitated FTO did not exhibit dramatic variation with different CTs. Although the levels of *FTO* mRNA in synchronized MEFs and mouse livers exhibited significant circadian oscillation (Fig. 4A), protein levels of FTO in synchronized MEFs and mouse livers showed no oscillation (Fig. 4B).

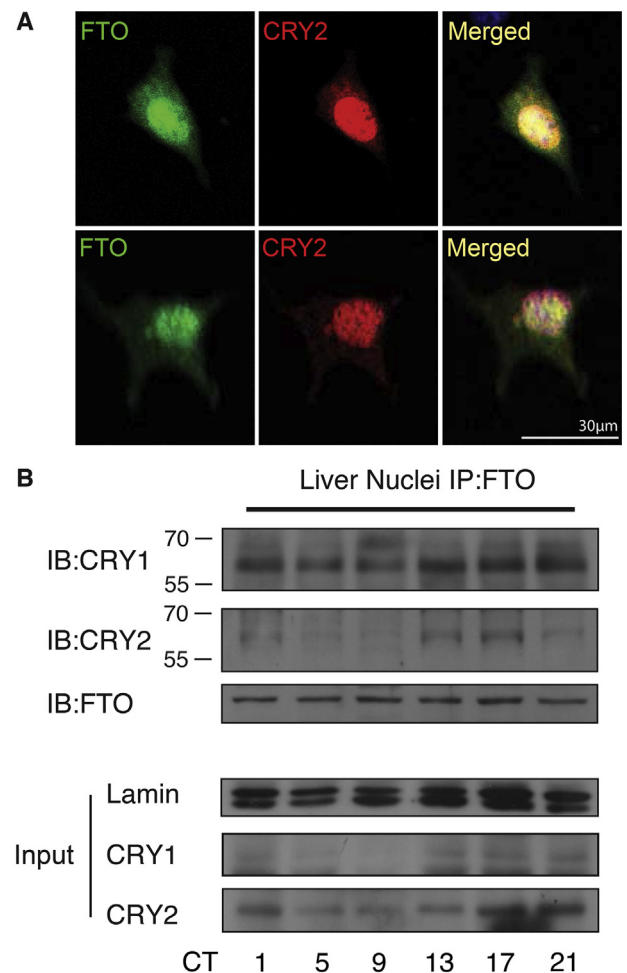


Fig. 3. FTO binds to CRY1/2 in a circadian manner. (A) Colocalization of GFP-tagged FTO with CRY2 in NIH-3T3 cells. (B) Liver extracts from CT 1, 5, 9, 13, 17, and 21 were immunoprecipitated with antibodies against FTO. Immunoprecipitates and input were analyzed by western blotting and probed for the indicated proteins. Each time point represents liver nuclei from six mice.

3.3. Molecular rhythms in FTO deficient mice

Since FTO deficient mice had a prolonged circadian period and altered responses to light, we predicted that the circadian gene expression patterns would be altered in these mice. To test this prediction, we collected livers from wild-type and FTO deficient mice at CT 1 and CT 13 during the first day in DD to

determine the expression levels of the core clock genes *PER1*, *PER2*, *CRY1*, *CRY2*, *Rev-Erb α* (*NR1D1*), *BMAL1*, and *CLOCK* (Fig. 4C). *PER1*, *PER2*, *CRY2*, *Rev-Erb α* , and *BMAL1* genes all exhibited significant circadian differences in mRNA levels at CT 1 and CT 13 in wild-type mice. Additionally, mRNA levels of *PER1*, *PER2*, *CRY2*, *Rev-Erb α* , and *BMAL1* genes also varied significantly in FTO deficient mice ($P < 0.05$). Moreover, the mRNA levels of *PER1*,

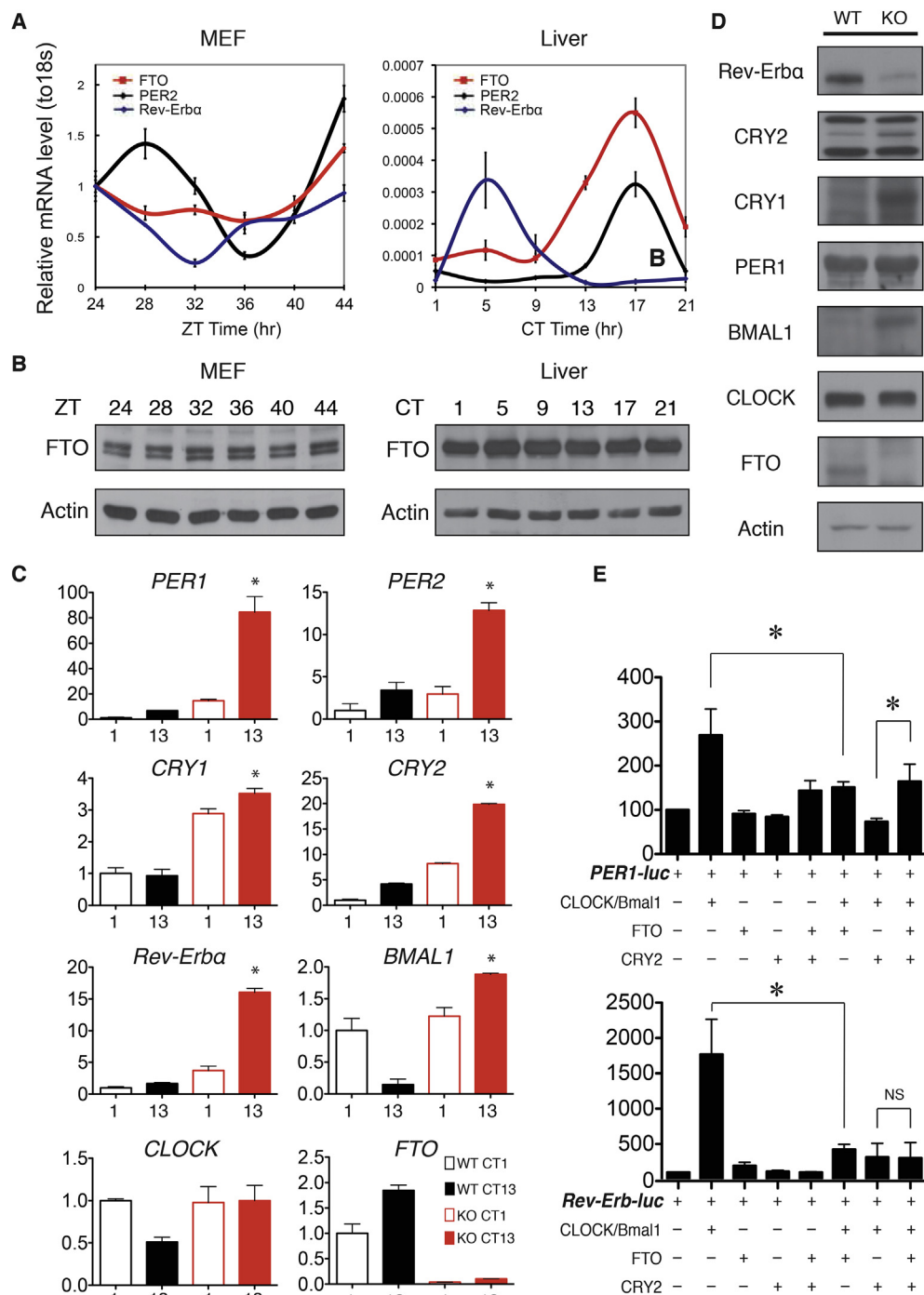


Fig. 4. Molecular rhythms in the livers of FTO deficient mice. (A) Circadian expression of *FTO* mRNA in synchronised MEFs by serum shock and in mouse livers. Plotted values are the mean \pm SD from three independent experiments. (B) *FTO* protein levels in synchronised MEFs by serum shock and in mouse livers. (C) The expression of core clock genes in the livers of WT and FTO deficient mice. Livers were collected at CT 1 and CT 13 on the first day in DD, and mRNA levels were determined by real-time PCR. Each point is the mean \pm SD of three mice. (D) Clock protein levels were altered in FTO deficient mice. Western blot analysis of Rev-Erb α , CRY2, CRY1, PER1, BMAL1, CLOCK, and FTO in the livers of WT and FTO deficient mice at CT 13. (E) NIH-3T3 cells were cotransfected with *PER1* or *Rev-Erb α* reporters in the presence (+) or absence (–) of expression plasmids, CLOCK, BMAL1, FTO, and CRY2. Each value is the mean \pm SD of three replicates. * $P < 0.05$. The results shown are representative of three independent experiments.

mPER2, *CRY1*, *CRY2*, *Rev-Erb α* , and *BMAL1* in FTO deficient mice were significantly higher than those in wild-type mice (Fig. 4C). We also examined various clock proteins in the livers of wild-type and FTO deficient mice at CT 13. Consistent with the changes in mRNA levels, *CRY1*, *CRY2*, and *BMAL1* protein levels were significantly elevated in FTO deficient mice (Fig. 4D). However, although *Rev-Erb α* mRNA expression was increased in FTO deficient mice, *Rev-Erb α* protein accumulation was actually lower in these mice. *CLOCK* and *PER1* protein accumulations were similar in wild-type and FTO deficient mice (Fig. 4D). These results suggested that FTO deficient mice had functioning molecular clocks, but exhibited changes in clock-related gene expression.

In addition to its function in *N*⁶-methyladenosine (*m*⁶A) in RNA, FTO has been shown to act as a transcriptional co-activator that enhances the transactivation potential of the CCAAT/enhancer binding proteins (C/EBPs). To test whether changes in the expression of circadian clock genes occurred through a transcriptional co-activation mechanism, we investigated whether FTO influenced *CLOCK:BMAL1*-mediated transcription in *mPER1* or *mRev-Erb α* promoters in cultured NIH-3T3 cells using a luciferase reporter-based system. Consistent with previous reports, *CRY2* inhibited the transcription activation by *CLOCK:BMAL1* heterodimers. Indeed, FTO overexpression repressed the transcriptional activation of the *mPER1* and *mRev-Erb α* promoters by *CLOCK:BMAL1* (Fig. 4E). In *mPER1* promoters, co-transfection of *CRY2* and FTO had higher luciferase activity compared to transfection of *CRY2* alone. In *mRev-Erb α* promoters, co-transfection of *CRY2* and FTO had similar luciferase activity compared to transfection of *CRY2* or FTO alone (Fig. 4E).

4. Discussion

In this study, we found that FTO repressed the transactivation activity of *CLOCK:BMAL1* heterodimers on clock genes. FTO deficiency resulted in abnormal clock genes accumulations and resulted in prolonged circadian periods and altered responses to light in mice. FTO deficient mice had overall period lengths that were ~18 min longer than those of wild-type mice. This result was not consistent with the wheel-running study in mice with FTO-overexpression, which revealed no differences in the period length compared to wild-type mice [7]. However, the prolonged period lengths with FTO deficiency were reminiscent of a recent study in which inhibition of RNA methylation with 3-deazaadenosine or silencing of the *m*⁶A methylase *Mettl3* were sufficient to elicit circadian period elongation and RNA processing delay [23]. The inconsistency between prolonged period lengths in inhibition of *m*⁶A demethylase FTO and methylase *Mettl3* and normal period lengths in FTO-overexpressing mice suggests distinct roles of FTO and implies that FTO may exert different effects on RNA methylomes from other methylases and demethylases.

The decreased *CLOCK:BMAL1* transactivation activity by overexpression of FTO implied that FTO also regulates circadian transcription-translation negative-feedback loop (TTFL). Since FTO is a RNA demethylase, it may also affect circadian rhythm through regulation of RNA methylation. It also suggested that FTO could have more complex functions rather than only RNA demethylase. Involvement of circadian rhythm modulation is strong evidence that FTO has boarder functions than body weight regulation alone.

The interaction between FTO and *CRY1/2* provides a strong support that FTO is involved in circadian rhythm control. FTO deficient mice had lower *Rev-Erb α* but higher *CRY1/2* protein levels with higher *Rev-Erb α* and *CRY1/2* mRNA levels compared to wild-type mice. Compared to transfection with *CRY2* alone, co-transfection of *CRY2* and FTO had significant different effects on

mPER2 promoters. On *mRev-Erb α* promoters, co-transfection with *CRY2* and FTO had similar effects when compared transfection with FTO alone. These evidences support interactions between FTO and *CRY1/2* have gene-specific effects. We reasoned that FTO-*CRY1/2* interactions could have two possible functions. First, the interaction between FTO and *CRY1/2* may have non-circadian functions, such as translational control or mTOR signalings or RNA demethylation. Second, FTO is enriched in various nuclear speckle-like structures and the interaction between FTO and *CRY1/2* could be dynamic and affected by different conditions. Since FTO shuttles between the cytoplasm and nucleus as *CRY1/2* does [24], their interaction could be dynamic and exerts important role in endoplasmic reticulum or mitochondria. Future studies will be needed to dissect the role between FTO and *CRY1/2*.

Author information

The authors declare no competing financial interests.

Acknowledgments

C.Y.W. received support from the National Health Research Institute (NHRI-EX100-9925SC), National Science Council (101-2314-B-182A-009, 101-2314-B-182A-098-MY3), and Chang Gung Memorial Hospital (CMRPG3B1643, CMRPG3C1762, CMRPG3D0581, and CMRPG3D1002). M.S.W. received support from National Science Council (103-2314-B-182A-092-MY3). S.S.S. received support from Chang Gung Memorial Hospital (CMRPG3C0722). We thank Jenn-Hwai Yang and Chien-Hsiun Chen at Academia Sinica for statistics, and Yu-Shien Ko at the microscope core laboratory of Chang Gung Memorial Hospital for help with the confocal microscopy study. Mei-Hsiu Lin, Yu-Jung Hu, and Hui-Ting Su provided technical supports.

Appendix A. Supplementary data

Supplementary data related to this article can be found at <http://dx.doi.org/10.1016/j.bbrc.2015.07.046>.

Transparency document

Transparency document related to this article can be found online at <http://dx.doi.org/10.1016/j.bbrc.2015.07.046>.

References

- [1] T. Gerken, C.A. Girard, Y.C. Tung, C.J. Webby, V. Saudek, K.S. Hewitson, G.S. Yeo, M.A. McDonough, S. Cunliffe, L.A. McNeill, J. Galvanovskis, P. Rorsman, P. Robins, X. Prieur, A.P. Coll, M. Ma, Z. Jovanovic, I.S. Farooqi, B. Sedgwick, I. Barroso, T. Lindahl, C.P. Ponting, F.M. Ashcroft, S. O'Rahilly, C.J. Schofield, The obesity-associated FTO gene encodes a 2-oxoglutarate-dependent nucleic acid demethylase, *Science* 318 (2007) 1469–1472.
- [2] T.M. Frayling, N.J. Timpson, M.N. Weedon, E. Zeggini, R.M. Freathy, C.M. Lindgren, J.R. Perry, K.S. Elliott, H. Lango, N.W. Rayner, B. Shields, L.W. Harries, J.C. Barrett, S. Ellard, C.J. Groves, B. Knight, A.M. Patch, A.R. Ness, S. Ebrahim, D.A. Lawlor, S.M. Ring, Y. Ben-Shlomo, M.R. Jarvelin, U. Sovio, A.J. Bennett, D. Melzer, L. Ferrucci, R.J. Loos, I. Barroso, N.J. Wareham, F. Karpe, K.R. Owen, L.R. Cardon, M. Walker, G.A. Hitman, C.N. Palmer, A.S. Doney, A.D. Morris, G.D. Smith, A.T. Hattersley, M.I. McCarthy, A common variant in the FTO gene is associated with body mass index and predisposes to childhood and adult obesity, *Science* 316 (2007) 889–894.
- [3] R.J.F. Loos, G.S.H. Yeo, The bigger picture of FTO-the first GWAS-identified obesity gene, *Nat. Rev. Endocrinol.* 10 (2014) 51–61.
- [4] T.D. Müller, M.H. Tschöp, S. Hofmann, Emerging function of fat mass and obesity-associated protein (fto), *PLoS Genet.* 9 (2013) e1003223.
- [5] S. Smemo, J.J. Tena, K.-H. Kim, E.R. Gamazon, N.J. Sakabe, C. Gómez-Marín, I. Aneas, F.L. Credidio, D.R. Sobreira, N.F. Wasserman, J.H. Lee, V. Puviindran, D. Tam, M. Shen, J.E. Son, N.A. Vakili, H.-K. Sung, S. Naranjo, R.D. Acemel, M. Manzanera, A. Nagy, N.J. Cox, C.-C. Hui, J.L. Gomez-Skarmeta, M.A. Nobrega, Obesity-associated variants within FTO form long-range

- functional connections with IRX3, *Nature* (2014) 1–17.
- [6] G. Stratigopoulos, J.F. Martin Carli, D.R. O'Day, L. Wang, C.A. Leduc, P. Lanzano, W.K. Chung, M. Rosenbaum, D. Egli, D.A. Doherty, R.L. Leibel, Hypomorphism for RPGRIP1L, a ciliary gene vicinal to the FTO locus, causes increased adiposity in mice, *Cell Metab.* 19 (2014) 767–779.
 - [7] C. Church, L. Moir, F. McMurray, C. Girard, G.T. Banks, L. Teboul, S. Wells, J.C. Bruning, P.M. Nolan, F.M. Ashcroft, R.D. Cox, Overexpression of Fto leads to increased food intake and results in obesity, *Nat. Genet.* 42 (2010) 1086–1092.
 - [8] S. Boissel, O. Reish, K. Proulx, H. Kawagoe-Takaki, B. Sedgwick, G.S. Yeo, D. Meyre, C. Golzio, F. Molinari, N. Kadhon, H.C. Etchevers, V. Saudek, I.S. Farooqi, P. Froguel, T. Lindahl, S. O'Rahilly, A. Munnich, L. Colleaux, Loss-of-function mutation in the dioxygenase-encoding FTO gene causes severe growth retardation and multiple malformations, *Am. J. Hum. Genet.* 85 (2009) 106–111.
 - [9] J. Fischer, L. Koch, C. Emmerling, J. Vierkotten, T. Peters, J.C. Bruning, U. Ruther, Inactivation of the Fto gene protects from obesity, *Nature* 458 (2009) 894–898.
 - [10] P.K. Olszewski, R. Fredriksson, J.D. Eriksson, A. Mitra, K.J. Radoska, B.A. Gosnell, M.N. Solvang, A.S. Levine, H.B. Schioth, Fto colocalizes with a satiety mediator oxytocin in the brain and upregulates oxytocin gene expression, *Biochem. Biophys. Res. Commun.* 408 (2011) 422–426.
 - [11] P. Gulati, M.K. Cheung, R. Antrobus, C.D. Church, H.P. Harding, Y.C. Tung, D. Rimmington, M. Ma, D. Ron, P.J. Lehner, F.M. Ashcroft, R.D. Cox, A.P. Coll, S. O'Rahilly, G.S. Yeo, Role for the obesity-related FTO gene in the cellular sensing of amino acids, *Proc. Natl. Acad. Sci. U. S. A.* 110 (2013) 2557–2562.
 - [12] E. Karra, O.G. O'Daly, A.I. Choudhury, A. Yousseif, S. Millership, M.T. Neary, W.R. Scott, K. Chandarana, S. Manning, M.E. Hess, H. Iwakura, T. Akamizu, Q. Millet, C. Gelegen, M.E. Drew, S. Rahman, J.J. Emmanuel, S.C.R. Williams, U.U. Rüther, J.C. Brüning, D.J. Withers, F.O. Zelaya, R.L. Batterham, A link between FTO, ghrelin, and impaired brain food-cue responsivity, *J. Clin. Invest.* 123 (2013) 3539–3551.
 - [13] G. Jia, Y. Fu, X. Zhao, Q. Dai, G. Zheng, Y. Yang, C. Yi, T. Lindahl, T. Pan, Y.G. Yang, C. He, N6-methyladenosine in nuclear RNA is a major substrate of the obesity-associated FTO, *Nat. Chem. Biol.* 7 (2011) 885–887.
 - [14] C.B. Green, J.S. Takahashi, J. Bass, The meter of metabolism, *Cell* 134 (2008) 728–742.
 - [15] C.L. Partch, C.B. Green, J.S. Takahashi, Molecular architecture of the mammalian circadian clock, *Trends Cell Biol.* 24 (2014) 90–99.
 - [16] J. Bass, J.S. Takahashi, Circadian integration of metabolism and energetics, *Science* 330 (2010) 1349–1354.
 - [17] M.E. Hughes, J.B. Hogenesch, K. Kornacker, JTK_CYCLE: an efficient nonparametric algorithm for detecting rhythmic components in genome-scale data sets, *J. Biol. Rhyth.* 25 (2010) 372–380.
 - [18] G. Asher, D. Gatfield, M. Stratmann, H. Reinke, C. Dibner, F. Kreppel, R. Mostoslavsky, F.W. Alt, U. Schibler, SIRT1 Regulates Circadian Clock Gene Expression through PER2 Deacetylation, *Cell* 134 (2008) 317–328.
 - [19] J.P. Etchegaray, X. Yang, J.P. DeBruyne, A.H. Peters, D.R. Weaver, T. Jenuwein, S.M. Reppert, The polycomb group protein EZH2 is required for mammalian circadian clock function, *J. Biol. Chem.* 281 (2006) 21209–21215.
 - [20] M. Akashi, T. Takumi, The orphan nuclear receptor RORalpha regulates circadian transcription of the mammalian core-clock Bmal1, *Nat. Struct. Mol. Biol.* 12 (2005) 441–448.
 - [21] S.H. Yoo, S. Yamazaki, P.L. Lowrey, K. Shimomura, C.H. Ko, E.D. Buhr, S.M. Sieppka, H.K. Hong, W.J. Oh, O.J. Yoo, M. Menaker, J.S. Takahashi, PERIOD2::LUCIFERASE real-time reporting of circadian dynamics reveals persistent circadian oscillations in mouse peripheral tissues, *Proc. Natl. Acad. Sci. U. S. A.* 101 (2004) 5339–5346.
 - [22] J.A. Mohawk, C.B. Green, J.S. Takahashi, Central and peripheral circadian clocks in mammals, *Annu. Rev. Neurosci.* 35 (2012) 445–462.
 - [23] J.-M. Fustin, M. Doi, Y. Yamaguchi, H. Hida, S. Nishimura, M. Yoshida, T. Isagawa, M.S. Morioka, H. Kakeya, I. Manabe, H. Okamura, RNA-methylation-dependent RNA processing controls the speed of the circadian clock, *Cell* 155 (2013) 793–806.
 - [24] P. Gulati, E. Avezov, M. Ma, R. Antrobus, P. Lehner, S. O'Rahilly, G.S. Yeo, Fat mass and obesity-related (FTO) shuttles between the nucleus and cytoplasm, *Biosci. Rep.* 34 (2014).